Journal of Organometallic Chemistry, 229 (1982) 229—245
Elsevier Sequoia S.A., Lausanne — Printed in The Netherlands

EXTENDED HÜCKEL MOLECULAR ORBITAL CALCULATIONS ON FUSED PENTAGONAL BIPYRAMIDAL METALLOCARBORANES CONTAINING WEDGE LIGANDS SUCH AS B—H, Sn, OR Ge

MARIA J. CALHORDA and D. MICHAEL P. MINGOS *

Inorganic Chemistry Laboratory, University of Oxford, South Parks Road, Oxford OX1 3QR (Great Britain)

(Received November 23rd, 1981)

Summary

Extended Hückel Molecular Orbital calculations have been completed on sandwich complexes derived from the *nido*-pentagonal bipyramidal $B_6H_6^{4-}$ and $C_2B_4H_6^{2-}$ ligands and the results contrasted with those obtained for related sandwich compounds derived from the cyclopentadienyl ligand. The calculations have been used to explain the electronic factors which prevent the formation of stable bent sandwich compounds derived from pentagonal borane ligands, and the bonding in "wedge" bridged sandwich compounds such as **1** and **2**.

The skeletal geometries of many seemingly disparate cagelike molecules have been rationalised and indeed sometimes predicted by a set of simple empirical electron counting rules described collectively as the Polyhedral Skeletal Electron Pair Theory [1—6]. These rules have their deficiencies, however, and in previous papers we have indicated some of the electronic factors leading to the breakdown of these electron counting rules and have accounted, for example, for the "slip" distortions in electron rich metallocarboranes [7—10]. Grimes and his coworkers [11,12] have reported some novel metallocarboranes which consist of two pentagonal bipyramidal units fused at a common iron atom with an additional group capping triangular faces on both polyhedra simultaneously. In **1** the molecule contains a direct iron—cobalt bond since the Co(η-C_5H_5) moiety is located in an equatorial position on one of the pentagonal rings and the additional B—H unit caps two triangular faces, one from each of the pentagonal bipyramidal polyhedra. In **2** there is only one transition metal atom and it is the Group IV atoms (Ge or Sn) which occupy the double capping or wedge position. Compounds of the type **1** and **2** are not readily explained in terms of the Polyhedral Skeletal Electron Pair Theory and alternative qualitative explanations have been proposed to describe the bonding in such complexes. Grimes [12] has suggested that in **1** and **2** there is a deficiency of two electrons relative

0022-328X/82/0000—0000/$02.75

to that required to support the presence of two fused pentagonal bipyramids, which causes the B—H group in 1 and the Group IV atom in 2 to adopt a double capping position between the pentagonal bipyramids. This represents

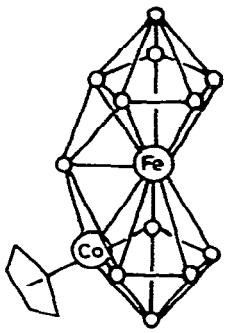

$C_4B_8H_8Fe(Co(\eta\text{-}C_5H_5))$

(1)

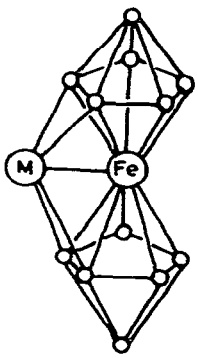

M = Sn or Ge

$C_4B_8H_8Fe(Sn)$

(2)

an extension of the capping principle [13] which states that a capping group may be introduced without extending the number of skeletal electron pairs required to support the structure. King et al. [14] have proposed an alternative graph theoretical explanation, which describes the bonding of the double capping B—H group in terms of a radial interaction between B—H and a non-bonding orbital on the iron atom which is complemented by interactions between the remaining *p* orbitals of the B—H unit with the surface orbitals of the two pentagonal bipyramidal units. In order to clarify the bonding in such molecules we have completed extended Hückel molecular orbital calculations on this class of molecule.

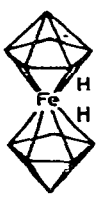

(3)

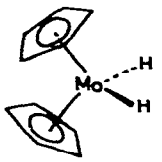

(4)

Although it has become common practice to view 1 and 2 as polyhedral entities they may also be considered as sandwich compounds derived from the relevant carborane or metallocarborane *nido*-pentagonal pyramidal ligands. This analogy is particularly pertinent when considering the bonding in $[FeH_2(\eta\text{-}C_2B_4H_6)_2]$ (3) [15], since it raises a separate question of why 3 does not adopt the bent sandwich structure observed in the isoelectronic $[MoH_2(\eta\text{-}C_5H_5)_2]$ complex (4) [16] rather than the more symmetrical structure illustrated in 3. The rings in 3 are very close to being parallel and are inclined only by 8°, whereas in 4 they are inclined by more than 40°. Since this structural dif-

ference has a bearing on understanding the formation of wedge bridged compounds such as **1** and **2** the electronic origins of this problem are also analysed in this publication.

Methods of calculation

All the calculations were made using the extended Hückel method [17,18]. The basis sets for the iron and cobalt atoms consisted of 3*d*, 4*s*, and 4*p* orbitals. The *s* and *p* orbitals were described by single Slater type wave functions and the *d* orbitals were taken as contracted linear combinations of two Slater type wave functions. The metal orbital exponents for the 3*d* [19], 4*s* and 4*p* [20, 21] atomic orbitals were taken from the literature. The parameters for the extended Hückel calculations are summarised in Table 1.

The calculations were made on the ICL 2900 computer at the Oxford University Computing Service using the ICON8 program developed by Hoffmann and his coworkers at Cornell University [17,18]. Calculations were made on the model compounds $[Fe(B_6H_6)_2]^{6-}$, $[FeH_2(B_6H_6)_2]^{4-}$, and $[Fe(BH)(B_6H_6)_2]^{4-}$. The B_6H_6 fragment was idealised as a *nido*-, C_{5v}, pyramidal fragment with dimensions $B_{eq} - B_{ax} = 1.73$ Å, $B_{eq} - B_{eq} = 1.69$ Å and B—H = 1.200 Å. The iron atom was placed at a distance of 2.17 Å from the two pentagonal borane cages.

The dimensions for the ferrocene molecule (C—C = 1.42 Å, C—H = 1.1 Å and Fe—C = 2.05 Å) were taken from published data [22]. In the corresponding hydrido complexes Fe—H was set equal to 1.60 Å and the H—Fe—H bond angle equal to 80°, except in those calculations where the hydrido ligand bridges an FeBB face. In these cases Fe—H was set equal to 1.56 Å, and set to lie 0.780 Å above the triangular face. In the B—H capped compounds the B—H fragment was placed 1.91 Å from the iron atom.

All calculations were performed using the modified Wolfsberg—Helholtz formula described in ref. 23.

TABLE 1

PARAMETERS FOR EXTENDED HÜCKEL CALCULATIONS

	Orbital	Slater exponent	H_{ii} (eV)	Ref.
H	1*s*	1.300	—13.60	18
B	2*s*	1.300	—15.20	18
	2*p*	1.300	—8.50	18
C	2*s*	1.625	—21.40	18
	2*p*	1.625	—11.40	18
Fe	4*s*	1.900	—9.17	20,21
	4*p*	1.900	—5.37	20,21
Co	4*s*	2.000	—8.54	20,21
	4*p*	2.000	—4.76	20,21

d wavefunctions

orbital		H_{ii} (eV)	ξ_1	c_1	ξ_2	c_2	Ref.
Fe	3*d*	—12.70	5.35	0.5366	1.80	0.6678	19,21
Co	3*d*	—12.11	5.55	0.6060	2.10	0.6060	19,21

Results and discussion

As in previous calculations which we have reported on metallocarboranes [7—10] the following strategy has been adopted for analysing the bonding. Initially the calculations were completed for the isoelectronic borane analogues, in order to maximise the symmetries of the molecules and assist in the delineation of the important electronic effects, then the effects of the carbon and metallocyclopentadienyl substituents were evaluated as perturbations on the general bonding model so developed.

Figure 1 illustrates the frontier molecular orbitals of the *nido*-pentagonal bipyramidal B_6H_6 fragment. As we have noted previously the frontier molecular orbitals of this fragment closely resemble those of the cyclopentadienyl anion [10], and in particular the $3e_2$, $3e_1$, and $4a_1$ molecular orbitals have nodal characteristics very similar to the π-molecular orbitals of $C_5H_5^-$. However, these orbitals have lower ionization energies for the borane fragment because of the lower electronegativity of boron compared to carbon. Figure 1 also indicates a significant difference between the frontier orbitals of B_6H_6 and C_5H_5. The former has a degenerate set of molecular orbitals ($2e_2$) which lies between $3e_1$ and $4a_1$ and are localised predominantly on the open face of the ligand. These orbitals, however, only interact weakly with the metal valence orbitals in sandwich complexes derived from this ligand because the boron *p* orbitals which contribute to this MO lie within the face of the ligand.

Figure 2 illustrates the molecular orbital interaction diagram for the symmetrical sandwich compound $[Fe(\eta\text{-}B_6H_6)_2]^{6-}$ with D_{5h} symmetry. The bonding closely resembles that for the more widely studied ferrocene molecule [23]. In particular the most significant interaction involving the metal *d* orbitals arises from the overlap between *xz*, *yz* and the ligand $3e_1''$ combination. The metal $x^2—y^2$ and *xy* orbitals enter into a weak four electron destabilising interaction with the ligand $2e_2'$ combination derived from $2e_2$ in Fig. 1. The metal z^2 orbital enters into a similar four electron destabilising interaction with $4a_1'$ (the symmetrical combination of the $4a_1$ orbital illustrated in Fig. 1),

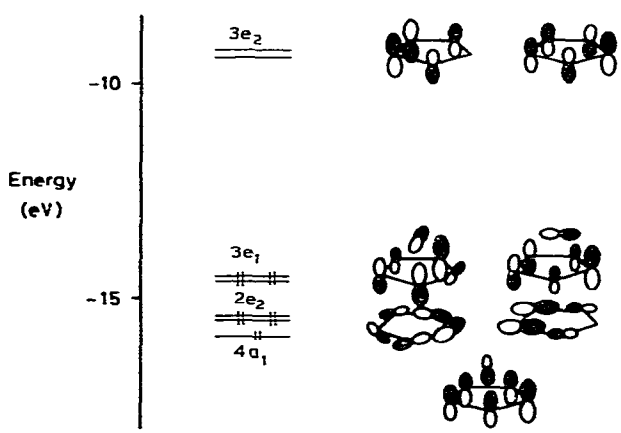

Fig. 1. Frontier molecular orbitals of the *nido*-$B_6H_6^{4-}$ pentagonal bipyramidal fragment.

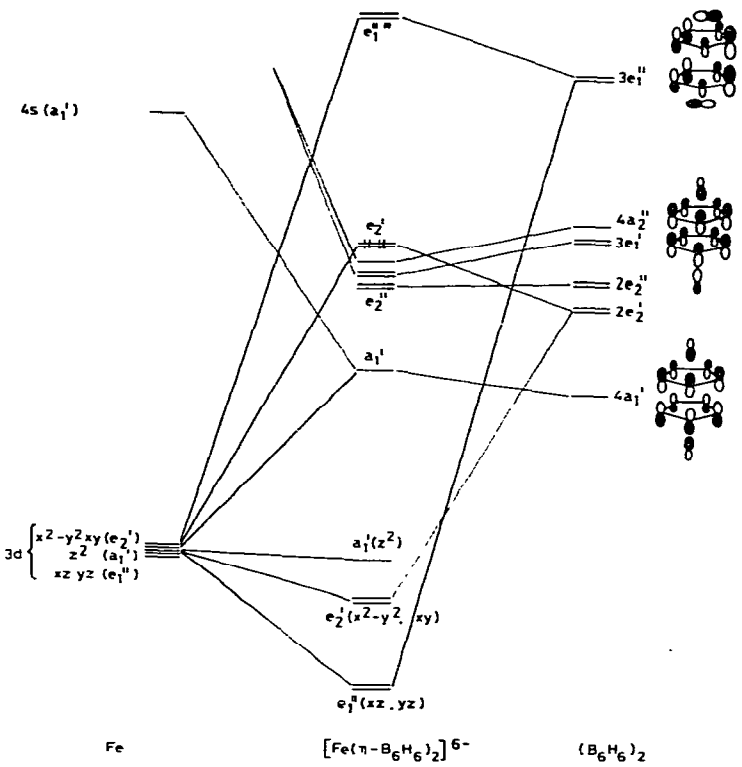

Fig. 2. Molecular orbital interaction diagram for $[Fe(B_6H_6)_2]^{6-}$ with D_{5h} symmetry. The highest occupied molecular orbital in this hypothetical anion by arrows.

however the antibonding component is stabilised somewhat by a significant overlap with the higher lying metal 4*s* orbital. The ligand e_1' combinations are also stabilised by interactions with the higher lying metal $4p_x$ and $4p_y$ orbitals. The ligand e_2'' orbitals remain non-bonding since there are no metal orbitals with matching symmetry,

The lower electronegativity of boron compared with carbon leads to significant differences in the bonding in $[Fe(\eta\text{-}B_6H_6)_2]^{6-}$ compared to ferrocene. In particular the highest occupied molecular orbitals in the former are localised predominantly in the ligand rather than the metal. The lowest unoccupied molecular orbital has e_1'' symmetry and represents the antibonding component of the ligand $3e_1''$ combination with the metal *xz*, *yz* orbitals. Again it is localised predominantly on the ligand (62%). Overall the metal—ligand interactions are stronger in the case of the borane sandwich compounds because of the electronegativity effect, and are reflected in the following overlap populations: Fe—B 0.232, and Fe—C 0.154.

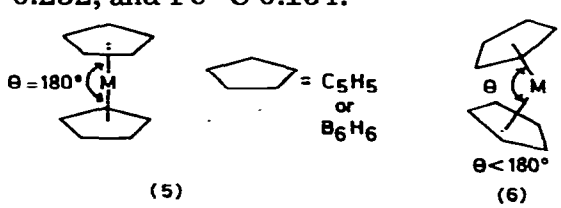

(5) (6)

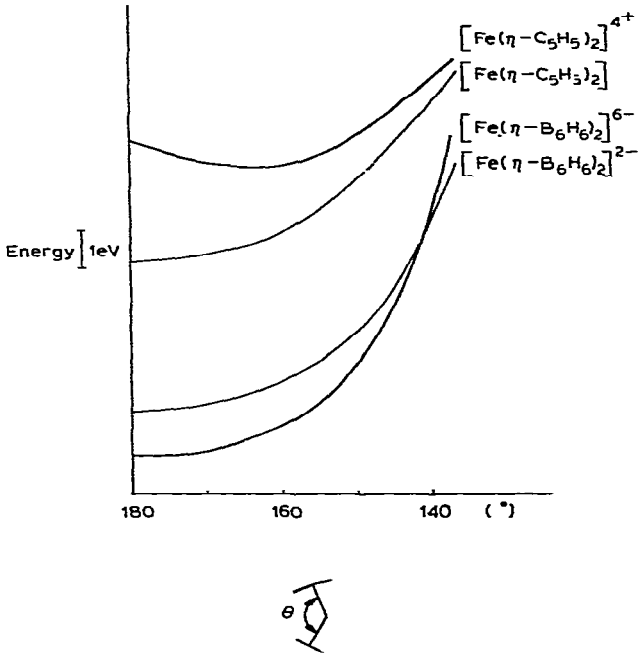

Fig. 3. Comparisons of the sums of the total one electron energies for $[Fe(B_6H_6)_2]^{n-}$, where $n = 6$ or 2, and $[Fe(C_5H_5)_2]^{m+}$, where $m = 0$ or 4, as a function of the interplanar ligand angle θ.

Figure 3 compares the energies of $[Fe(\eta\text{-}B_6H_6)_2]^{6-}$ and $[Fe(\eta\text{-}C_5H_5)_2]$ as the interplanar angle, θ, is reduced from 180° (parallel)(5) to 135° (bent)(6). The potential energy surface is substantially softer for ferrocene than the borane sandwich anion. There are two basic reasons for this. Firstly, there is a purely geometric reason arising from the fact that the C—C distance in the cyclopentadienyl complex of 1.42 Å is significantly shorter than the B—B distance of 1.69 Å in the borane complex anion. Consequently when the rings are bent back the boron atoms lying on the mirror plane and their associated hydrogen atoms move more closely together and stronger four electron destabilising interactions between the filled B—B bonding and B—H bonding molecular orbitals on the two rings are generated. These interactions are illustrated schematically in 7 and 8. Secondly, the weaker ring—metal interactions for ferrocene means that

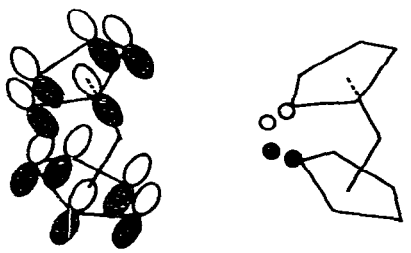

(7) (8)

less stabilization energy is lost when the rings are distorted away from their more symmetrical equilibrium arrangement.

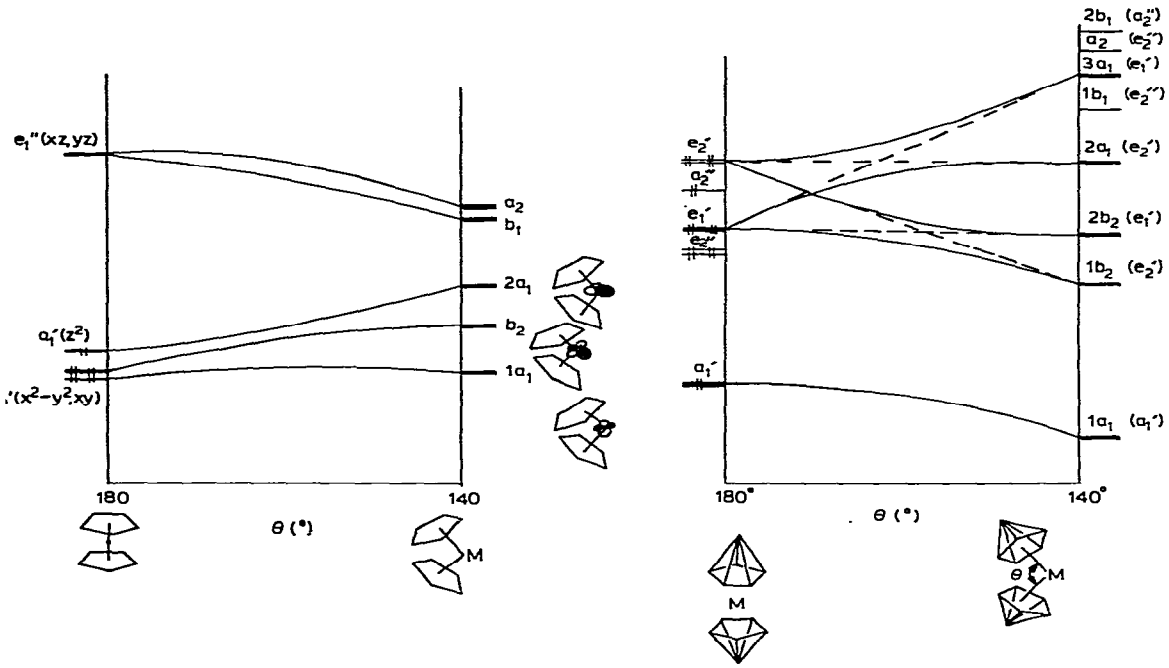

Fig. 4. Comparisons of the Walsh diagrams for the bending distortion in related metallocene (Fig. 4a) and metalloborane sandwich (Fig. 4b) complexes. For reasons of clarity only those curves for orbitals which mix extensively have been illustrated in Fig. 4b. The remaining orbitals derived from a_2'' and e_2'' are only shown for $\theta = 180^{\circ}$ and 136°.

The differences in the gradients of the potential energy surfaces become even more pronounced when four electrons are removed from the highest occupied molecular orbitals of the cyclopentadienyl and borane sandwich complexes to form $[Fe(\eta\text{-}C_5H_5)_2]^{4+}$ and $[Fe(\eta\text{-}B_6H_6)_2]^{2-}$, respectively. For the former the potential energy surface shows a minimum at $\theta = 160^{\circ}$ and an energy difference of only 0.66 eV separates the $\theta = 180^{\circ}$ and $\theta = 136^{\circ}$ geometries. This energy difference is significantly smaller than the typical metal—ligand bond energy and consequently it is possible to form a wide range of 18 electron bent sandwich complexes of the type $M(\eta\text{-}C_5H_5)_2L_2$ [24]. For the corresponding borane anion, $[Fe(B_6H_6)_2]^{2-}$, a large energy separation still separates the $\theta = 180^{\circ}$ and $\theta = 136^{\circ}$ geometries (5.48 eV) and it remains highly unfavourable to form bent borane sandwich complexes of the type $[Fe(\eta\text{-}B_6H_6)_2L_2]$. The reasons for the maintenance of a steep potential energy surface for the borane anion may be appreciated by comparing the Walsh diagrams in Fig. 4 for the bending distortion in the two classes of complex. In a d^6 cyclopentadienyl complex the highest occupied molecular orbitals are localised predominantly on the metal and are essentially non-bonding, i.e. $a_1'(z^2)$ and $e_2'(xy, x^2-y^2)$ in Fig. 4a. As θ is decreased these orbitals mix more extensively with lower lying ligand orbitals and consequently become more antibonding. In addition substantial mixing between the $a_1(z^2)$ and $a_1(x^2-y^2)$ components, now permitted in the lower symmetry (C_{2v}) bent sandwich structure, occurs. This mixing has significant consequences for the bonding capabilities of bent sandwich fragments and

TABLE 2

COMPARISON OF THE ELECTRON DISTRIBUTIONS IN $Fe(C_5H_5)_2$ AND $Fe(B_6H_6)_2$ FRAGMENTS WITH θ 136°

$Fe(C_5H_5)_2$ Orbital	Composition, %	
	Ligands	Metal
$2a_1$	23	$48z^2$, 11x, $8x^2-y^2$, 5s
b_2	49	43xy, 8y
a_1	25	$57x^2-y^2$, $17z^2$
$Fe(B_6H_6)_2$ Orbital	Ligands	Metal
$3a_1$	65	$17z^2$, 14x, $2x^2-y^2$, 2s
$2b_2$	80	9xy, 11y
$2a_1$	70	$26z^2$, 4s

this aspect has been discussed in some detail by several groups [23—25]. The compositions of the relevant frontier orbitals of the bent metallocene fragment are summarised in Table 2.

For the borane anion the highest occupied molecular orbitals are localised predominantly on the ligands and although the bending distortion is associated with the more complicated Walsh diagram illustrated in Fig. 4b its important features can be qualitatively understood using simple perturbation theory arguments. Those molecular orbitals which are antisymmetric with respect to the horizontal mirror plane in the molecule, i.e. a_2'' and e_2'' are destabilised as the rings are bent because the out of phase inter-ring boron-boron overlap integrals increase (see 9 for example).

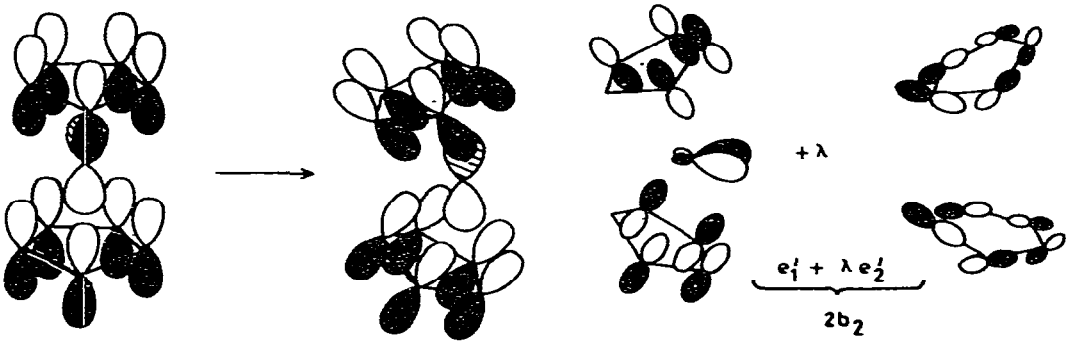

(9) (10)

Those orbitals which are symmetric with respect to the horizontal mirror plane, i.e. e_2' and e_1', each give rise to a_1 and b_2 components in the bent sandwich structure. The lower lying a_1 molecular orbital which has a significant amount of z^2 character also gives rise to an a_1 component. The b_2 components mix extensively: the higher lying $2b_2$ having 50% (e_1') and 28% (e_2') character and the lower lying $1b_2$ having 37% (e_1') and 53% (e_2') character. In addition the former has a much higher contribution from the metal xy (10%) and y

(11%) orbitals and consequently resembles more closely the b_2 orbital of the bent metallocene fragment. The relative contributions of the ligand and metal orbitals in the cyclopentadienyl and borane angular fragments are compared in Table 2. The $2b_2$ orbital, which is illustrated schematically in **10**, plays an important role in bonding between the bent metalloborane fragment and incoming ligands.

The a_1 component derived from e_2' does not change either its composition or energy greatly as a result of the bending distortion since it is primarily an in-plane orbital rather than an out-of-plane orbital and is noded at those boron atoms which are closest together in the bent structure (see **11**). In the Walsh diagram in Fig. 4b the orbital is labelled $2a_1$ in the bent geometry. The a_1 components derived from e_2', e_1' and a_1' mix extensively giving rise to the characteristic avoided crossing pattern in Fig. 4b. The mixing of the two lower lying molecular orbitals can be represented schematically by **12**.

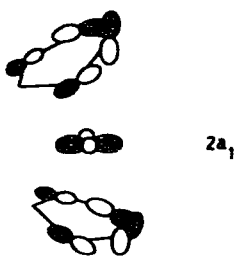

(11)

The higher lying orbital becomes more localised on the metal as the bending angle is decreased and has only 65% ligand character when $\theta = 136°$. It is this

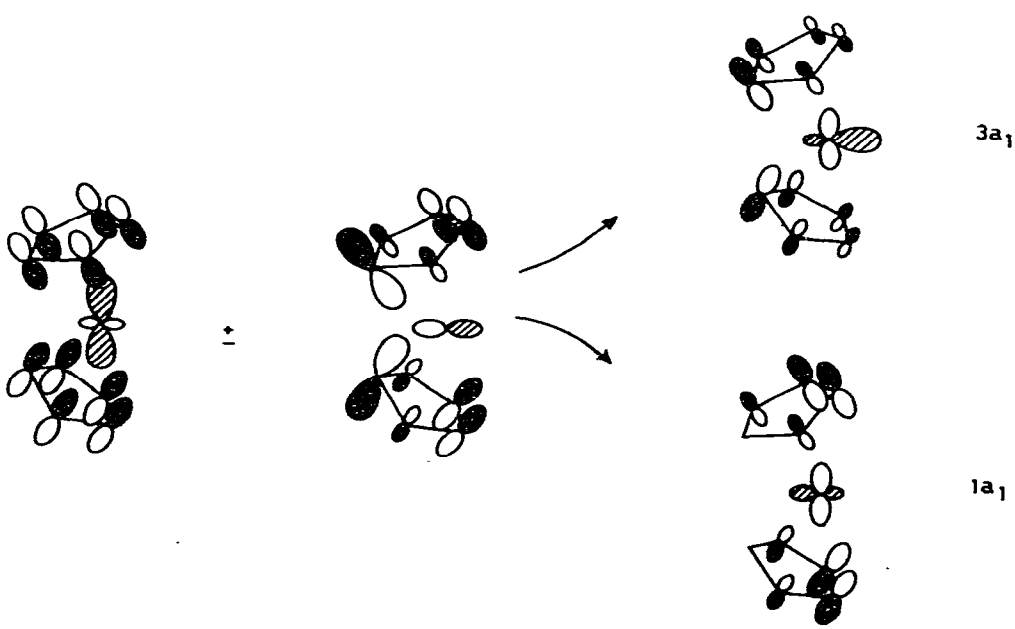

(12)

orbital which most closely approximates to the $2a_1$ molecular orbital of the bent cyclopentadienyl sandwich fragment (see Table 2 for a comparison of the relevant orbitals).

Comparison of the bonding in bent sanwich complexes derived from cyclopentadienyl and B_6H_6

The bent sandwich borane fragment $[Fe(\eta\text{-}B_6H_6)_2]^{2-}$ (6) utilises its $2b_2$ (10) and $3a_1$ (12) molecular orbitals in much the same way as that described previously for cyclopentadienyl bent sandwich compounds [24]. Figure 5 illustrates the

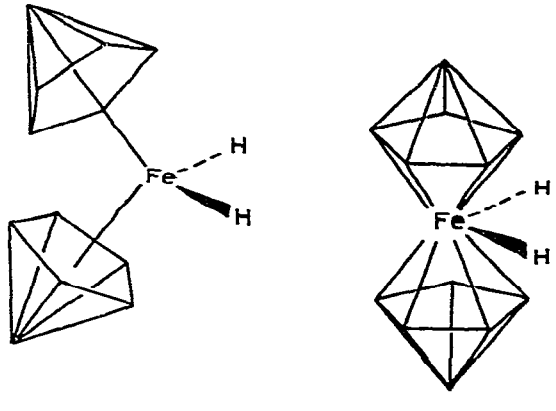

(13) (14)

interaction diagram for the formation of the dihydrido complex $[FeH_2(B_6H_6)_2]^{4-}$ (13) from the bent $[Fe(\eta\text{-}B_6H_6)_2]^{2-}$ fragment. The hydrido a_1 and b_2 linear combinations interact primarily with the metalloborane $3a_1$ and $2b_2$ molecular

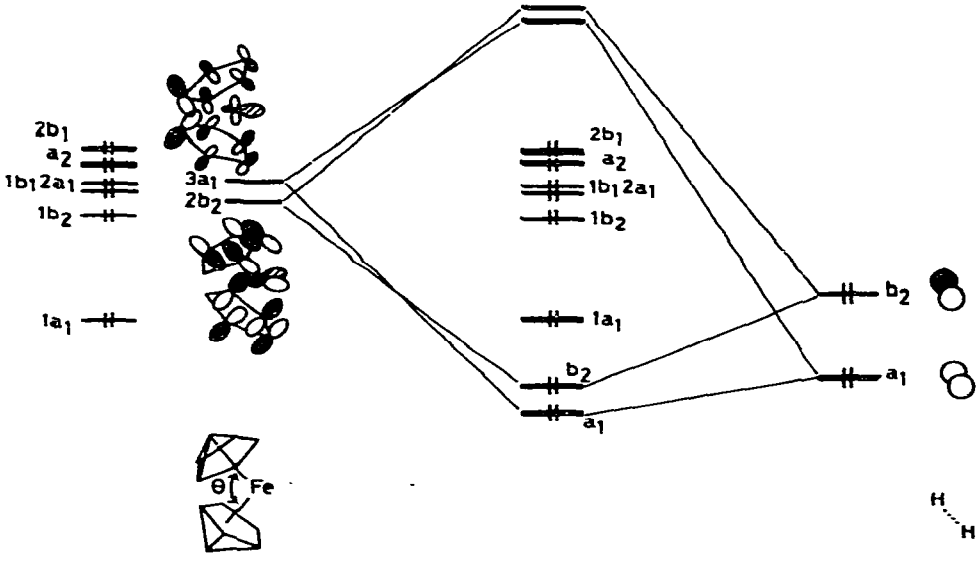

Fig. 5. Molecular orbital interaction diagram for $[FeH_2(B_6H_6)_2]^{4-}$ in the bent sandwich geometry with θ 136°.

orbitals. Clearly in terms of the total electron count such a structure is acceptable since the 18 valence electrons lead to a filling of all the bonding and non-bonding molecular orbitals. However, it is less stable than the alternative symmetrical structure 14 because the hydrido—metal interactions are less strong than those in the corresponding bent cyclopentadienyl sandwich compound. This results because the frontier orbitals are less localised on the metal. The interactions between the hydrido ligands and the cage atoms are significantly larger for the borane sandwich complex. This is effectively illustrated by the following computed overlap populations:

	$[FeH_2(B_6H_6)_2]^{4-}$	$[Fe(C_5H_5)_2]^{2+}$
Fe—H	0.425	0.487
B(or C)—H	0.091	0.044

The extended Hückel calculations suggest that the bent sandwich structure is favoured over the alternative symmetrical ($\theta = 180°$) structure by 1.3 eV in the case of the cyclopentadienyl complex. However, for the corresponding borane complex the opposite is true and the symmetrical sandwich structure 14 is 2.5

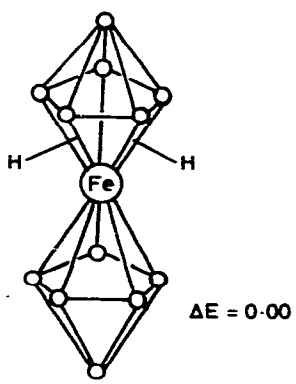

ΔE = 0·00

(15)

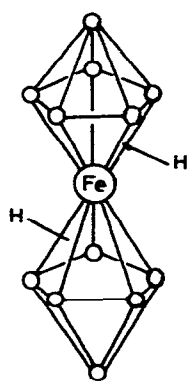

ΔE = 0·04 eV

(16)

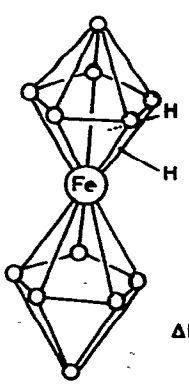

ΔE = 0·10 eV

(17)

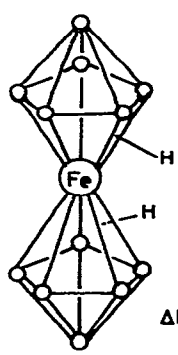

ΔE = 0·004 eV

(18)

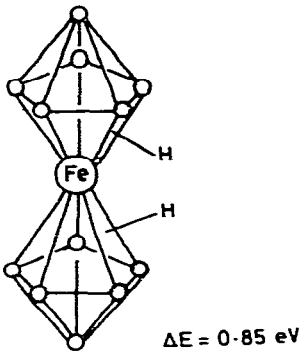

(19)

eV more stable than the bent structure **13** with $\theta = 136°$. Although this difference can in large measure be attributed to the greater energy required to distort the sandwich structure in the case of the borane complex, it is also influenced by the weaker metal—hydrogen bonding in the borane complex. This arises from the smaller degree of localisation of the frontier orbitals of the $[Fe(B_6H_6)_2]^{2-}$ fragment on the metal atom.

In the X-ray structural determination of $[FeH_2(\eta\text{-}C_2B_4H_6)_2]$ the hydrogen atoms could not be located directly but it was proposed on the basis of NMR evidence that the hydrogens reside on FeBB triangular faces. We have completed extended Hückel calculations on the alternative hydrido isomers **15** to **19** which satisfy this requirement. The structures **15** to **18** were found to have total energies within 0.1 eV of each other and consequently cannot be distinguished within this level of approximation. Only structure **19** with the two hydrogens in close proximity (H—H = 0.988 Å) was found to be energetically disfavoured. These results are compatible with the NMR studies which have indicated that in **3** the hydrogens are involved in a low energy fluxional process involving migration of the hydrogen atoms over the alternative FeBB triangular faces.

Interactions between the sandwich compounds and a double capping B—H fragment

The B—H fragment is characterised by a filled low lying outpointing hybrid orbital hy(s—x) of σ symmetry and a degenerate pair of empty boron p_y and p_z orbitals of π symmetry. Therefore, the B—H ligand potentially has a coordination chemistry akin to that of cylindrically symmetric π-acid ligands such as CO and should form multiple bonds with metal fragments having the appropriate vacant and filed orbitals. Indeed the possibility of boryne complexes is encouraged by the recent syntheses of stable carbyne complexes particularly by Fischer, Schrock and their coworkers [25,26].

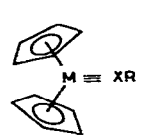

(20)

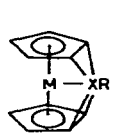

X = B or C

M = Re or Mo

(21)

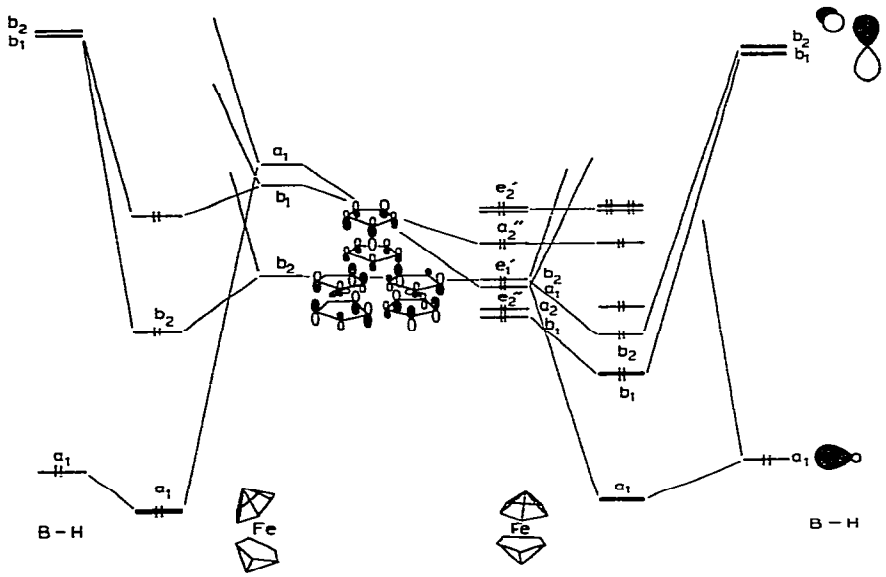

Fig. 6. Molecular orbital interaction diagram for the formation of a sandwich compound with a double capping wedge ligand. The right hand side of the figure illustrates the situation for θ 180° and the left hand side for θ 136°.

Furthermore since the carbonyl complex $Mo(CO)(\eta\text{-}C_5H_5)_2$ is well documentec the corresponding bent sandwich carbyne and boryne complexes $Mo(CR)(\eta\text{-}C_5H_5)_2$ and $Re(BR)(\eta\text{-}C_5H_5)_2$ (**20**) would appear to be electronically satisfactory. However, the results described above for $[FeH_2(\eta\text{-}B_6H_6)_2]^{4-}$ suggest that structure **21** might be an alternative structure for such sandwich compounds. Moreover, the related borane complexes **1** and **2** have been shown to have such a structure. Therefore, we have completed extended Hückel calculations for cyclopentadienyl and B_6H_6 sandwich complexes with B—H based on the geometries illustrated in **20** and **21**.

Figure 6 illustrates the relevant interaction diagrams for $[Fe(BH)(B_6H_6)_2]^{4-}$ in the alternative geometries **20** and **21**. For the more symmetrical sandwich structure (i.e. $\theta = 180°$) the B—H, a_1, hy(s—p_x) orbital interacts primarily with the a_1 component derived from e_1'. In addition there is a supplementary interaction with a lower lying a_1 orbital having a substantial degree of d_{z^2} character and this is schematically illustrated in **22**.

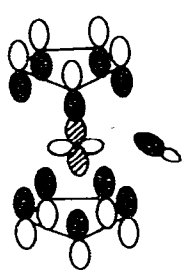

(22)

There is a considerable degree of B_{cap}—B_{cage} bonding involved as a result of these interactions since the a_1 component of e_1' is localised on the ligand to the extent of 77% and the lower lying a_1 orbital 45%. In order for these interactions to be stabilising it is necessary for the $[Fe(B_6H_6)_2]$ fragment to have an empty orbital in its non-bonding set, i.e. it must have an overall charge of 4—.

This forward donation component is supplemented by back donation components from filled orbitals on the $[Fe(B_6H_6)_2]$ fragment to the empty p_y and p_z orbitals of B—H. The B—H p_y orbital interacts in this fashion with the b_2 component of e_1' (see Fig. 6) and the B—H p_z orbital interacts primarily with the b_1 component of e_2'', which is localised exclusively on the B_6H_6 ligands, and to a lesser extent with the b_1 orbital derived from the orbital of a_2'' symmetry in the isolated sandwich compound. These back donation components also give rise to substantial B_{cap}—B_{cage} bonding since these orbitals are localised extensively on the borane ligands. This is confirmed by the computed overlap populations summarised below:

	$[Fe(BH)(B_6H_6)_2]^{4-}$	$[Fe(BH)(C_5H_5)_2]^{2+}$
Fe—BH	0.375	0.325
B_{cap}—B(or C)	0.356	0.168

In the related compound involving the cyclopentadienyl ligand structure **21** is less favoured because the frontier orbitals of the $Fe(C_5H_5)_2$ fragment are more stable and less localised on the ring atoms. The hy(s—p_x) B—H molecular orbital interacts effectively with the a_1 component of e_2' of $Fe(C_5H_5)_2$ forming the basis of the dative HB—Fe dative bond. The back donation component is, however, limited to an interaction between the b_2 component derived from $e_2'(x^2—y^2, xy)$ and the B—H p_y orbital. This interaction involves an $Fe(C_5H_5)_2$ orbital which is localised extensively on the metal and results in little B_{cap}—C bonding. The other B—H p orbital, p_z, finds no effective interaction since the $Fe(C_5H_5)_2$ fragment has no counterpart to the e_2'' orbital illustrated in Figure 6 and the a_2'' orbital of $[Fe(C_5H_5)_2]$ is much lower in energy and does not effectively back donate into the B—H p_z orbital. These effects are emphasized by the overlap populations given above for $[Fe(BH)(C_5H_5)_2]^{2+}$ which show strong bonding between Fe and B—H, but weak C—BH bonding.

As the rings are bent back to give structure **20** with $\theta' = 136°$ the borane capped complex $[Fe(BH)(B_6H_6)_2]^{4-}$ is destabilised by a substantial amount (4.4 eV). In part this large energy difference originates from the large energy required to bend back the pentagonal rings in the $[Fe(B_6H_6)_2]^{4-}$ fragment, but in addition there is a contribution from the weaker B—H_{cap}—B_{cage} interactions in the bent sandwich structure. In part this is compensated for by stronger Fe—B—H bonding but not completely. Figure 6 illustrates the effect of the bending distortion on the important frontier orbitals of $[Fe(B_6H_6)_2]$ and their interactions with the B—H fragment in the bent sandwich structure. Although the energy of the a_1 component of e_1' rises as a result of the bending distortion the Fe—B—H interaction is strengthened because of the rehybridisation and localization effects of the resultant $3a_1$ orbital illustrated in **12**. The back donation component resulting from the $2b_2$—p_y interaction also remains strong and gains

om the rehybridisation effects at the metal illustrated in **10**. These effects e reproduced by the following computed overlap populations:

–B–Fe(B_6H_6)$_2$	$\theta = 180°$	$\theta = 136°$
$(s-x)-a_1$	0.283	0.453
$-b_2$	0.125	0.165
$-b_1$	0.322	0.132

owever, the other back donation component originating from the overlap of rbitals of b_1 symmetry is reduced considerably. This interaction involved an rbital which was localised exclusively on the cage boron atoms when $\theta = 180°$ nd its overlap with the capping B–H p_z orbital is reduced considerably as the ngs are bent back.

For the related cyclopentadienyl complex the bent geometry with the onventional type of metal–boryne bonding is preferred to the wedge bridged ructure by 0.5 eV. This arises because the weaker HB–C interactions in the ent sandwich structure are compensated for by stronger Fe–B bonding since ie relevant frontier orbitals of the Fe(C_5H_5)$_2$ fragment are more localized on ie iron atom (see Table 2). The relatively soft calculated potential energy rface for the interconversion of structures **20** and **21** in the case of the yclopentadienyl–boryne complex leads to the interesting prediction that ich complexes and the related carbyne complexes may undergo a facile luxional process involving the making and breaking of B–H (or C–H)–cage onds.

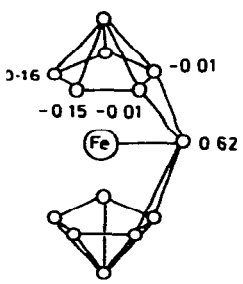

(23)

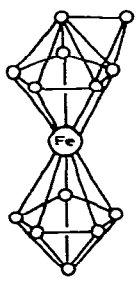

(24)

The computed atomic charges for [Fe(BH)(B_6H_6)$_2$]$^{4-}$ illustrated in **23** suggest hat overall the wedge B–H ligand is acting as a σ-donor rather than a π-acceptor since the capping atom bears an overall positive charge of +0.62 e. The symmetric charge distribution introduced into the pentagonal faces of the $_6H_6$ ligands also suggests on the basis of first order perturbation theory arguments the following site preferences for substituents. More electronegative olobal substituents such as C–H should occupy those negatively charged cage ositions farthest from the B–H capping ligand, whereas less electronegative ubstituents should occupy those positions adjacent to the capping B–H ligand. he structural determination completed on **1** which is isoelectronic with [Fe-BH)(B_6H_6)$_2$]$^{4-}$ (as far as the cage bonding is concerned) bears out these site

preference arguments. Furthermore, since a Sn or Ge atom is isolobal with B—H the bonding model developed above is readily applicable to the isoelectronic compounds illustrated in **2**.

As part of the analysis we also considered the alternative isoelectronic structure illustrated in **24** which has the B—H ligand capping a single BBB face rather than a wedge position. In agreement with considerations based on the capping principle [13] such a structure leads to a closed shell electronic configuration, however the structure is substantially (1.5 eV) less stable than the alternative wedge structure. The reason for this originates in the localisation of the frontier orbitals of $[Fe(B_6H_6)_2]^{4-}$ on the pentagonal faces of the ligands which leads to larger overlap integrals with the B—H group in the wedge rather than the capping position.

The structural determination of $[Fe(BH)(CoCpC_2B_3Me_2H_3)(C_2B_4Me_2H_4)]$ (**1**) has demonstrated that the wedge (or capping) B—H ligand is not bonded to the two pentagonal bipyramidal cages in a symmetrical fashion. In particular the BH_{wedge}—B distances to the cage not containing cobalt are exceptionally long (average 2.14 Å) and some 0.4 Å longer than the BH_{wedge}—B distance to the cage containing the cobalt atom. Therefore from a theoretical point of view it was necessary to establish whether this asymmetry is a general feature of wedge compounds or a specific feature of **1** which arises from the asymmetry introduced by the cobalt substituent. Calculations on the model compound $[Fe(BH)(B_6H_6)_2]^{4-}$ have demonstrated that the most stable structure is that shown in **21** with the BH ligand interacting in a symmetrical fashion with both pentagonal bipyramidal cages, suggesting that it is the effect of the cobalt substituent which is causing the asymmetric bonding. This is supported by a calculation on the model compound $[Fe(BH)(B_6H_6)(CoCpB_5H_5)]^{4-}$ which demonstrated that the overlap populations to the cage not containing cobalt were significantly smaller than that to the cobalt containing cage (see **25**). These asymmetric bonding effects can be readily appreciated using perturbation theory arguments in conjunction with the bonding model developed above.

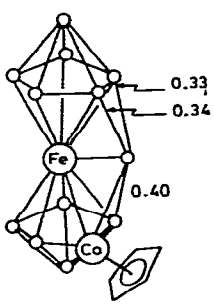

(25)

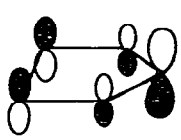

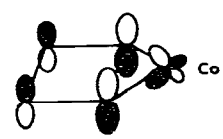

(26)

The introduction of the CoCp fragment into the B_6H_6 cage raises the degeneracy of the $3e_1$ orbital and the symmetric component illustrated in **26** lies approximately 1.8 eV higher in energy than the corresponding antisymmetric component. Similarly the energy of the antisymmetric component of $2e_2$ is raised by a similar amount. Consequently these molecular orbitals are able to interact more effectively with the p_z and p_y orbitals of the capping B—H ligand

leading to stronger bonding to the cobalt containing cage. The introduction of the cobalt substituent also has the effect of increasing the coefficients of the *p* orbitals of those boron atoms adjacent to cobalt (see 26) and thereby increasing the overlap with the capping B—H group. Therefore the bonding model developed above not only accounts for the total electron count in such molecules but also the observed distortions.

Acknowledgements

The Gulbenkian Foundation and the S.E.R.C. are thanked for financial support.

References

1 K. Wade, Adv. Inorg. Chem. Radiochem., 18 (1976) 1.
2 R.W. Rudolph, Acc. Chem. Res., 9 (1976) 446.
3 D.M.P. Mingos, Nature (London), Phys. Sci., 236 (1972) 99.
4 C.J. Jones, W.J. Evans,and M.F. Hawthorne, J. Chem. Soc. Chem. Commun., (1973) 543.
5 R.N. Grimes, Ann. N.Y. Acad. Sci., 239 (1974) 180.
6 R.B. King and D.H. Routhray, J. Amer. Chem. Soc., 99 (1977) 7834.
7 D.M.P. Mingos, J. Chem. Soc. Dalton Trans., (1977) 602.
8 D.M.P. Mingos, M.I. Frosyth and A.J. Welch, J. Chem. Soc. Dalton Trans., (1978) 1363.
9 D.M.P. Mingos and M.I. Forsyth, J. Organometal. Chem., 146 (1978) C37.
10 M.J. Calhorda, D.M.P. Mingos and A.J. Welch, J. Organometal. Chem., 228 (1982) 309.
11 W.M. Maxwell, E. Sinn, and R.N. Grimes, J. Amer. Chem. Soc., 98 (1976) 3490.
12 R.N. Grimes, Acc. Chem. Res., 11 (1978) 421.
13 D.M.P. Mingos, J. Chem. Soc. Dalton Trans., (1977) 610.
14 R.B. King, E.K. Nishimura and K.S.R. Veer, Inorg. Chem., 19 (1980) 2478.
15 J.R. Pipal and R.N. Grimes, Inorg. Chem., 18 (1979) 263.
16 A.J. Schultz, K.L. Sterarly, J.M. Williams, R. Mink, and G.D. Stuckey, Inorg. Chem., 16 (1977) 3303.
17 R. Hoffmann, J. Chem. Phys., 39 (1963) 1397.
18 R. Hoffmann and W.N. Lipscomb, J. Chem. Phys., 37 (1962) 3179; 37 (1962) 2872.
19 J.W. Richardson, W.C. Nieuwport, R.P. Powell and W.F. Edgell, J. Chem. Phys., (1962) 1057.
20 R.H. Summerville and R. Hoffmann, J. Amer. Chem. Soc., 98 (1976) 7240.
21 T.A. Albright, P. Hoffmann and R. Hoffmann, J. Amer. Chem. Soc., 99 (1977) 7546.
22 A. Haaland, Acc. Chem. Res., 12 (1979) 415.
23 J.H. Ammeter, H.-B. Burgi, J.C. Thibeault and R. Hoffmann, J. Amer. Chem. Soc., 100 (1978) 3686.
24 J.W. Lauher and R. Hoffmann, J. Amer. Chem. Soc., 98 (1976) 1729.
25 E.O. Fischer und U. Schubert, J. Organometal. Chem., 100 (1975) 59.
26 S.J. McLain, C.D. Wood, L.W. Messerle, R.R. Schrock, F.J. Hollander, W.J. Yongs and M.R. Churchill, J. Amer. Chem. Soc., 100 (1978) 5962.